euspen's 21st International Conference & Exhibition, Copenhagen, DK, June 2021
www.euspen.eu

Optical rotating torque sensor with nano newton-meter resolution based on a hanging torsion wire

Etienne Thalmann[1], Billy Nussbaumer[1], Simon Henein[1]

[1]*EPFL, Instant-Lab, Rue de la Maladière 71b, 2000 Neuchâtel, Switzerland*

etienne.thalmann@epfl.ch

Abstract

This article presents a novel torque measuring setup working in the nano newton-meter (10^{-9} Nm) range. The central novelty is a long (1 meter range) thin (diameter of a few tens of micrometers) metallic wire used instead of the relatively stiff torsion zone of the shaft of classical rotating torque sensors. This thin wire is made straight by placing it vertically and suspending a mass at its lower extremity. The very low torsional stiffness of the wire is determined by measuring the frequency of the torsional pendulum constituted by the wire and its hanging mass. The twist-angle of the wire is measured optically. The setup can be used to measure torques in static and rotating modes. The performance of this setup has been demonstrated by measuring the output torque of a modified mechanical watch gear train constituted of two 10:1 speed multiplying stages in series, driven by a commercial torque meter. With outputs torques ranging from $40 \cdot 10^{-9}$ to $160 \cdot 10^{-9}$ Nm, the measurements showed a linear input to output torque ratio of 108 for a total gear ratio of 100:1, corresponding to a load-dependent efficiency of 92.6%. The measured constant loss is $7.63 \text{ nN} \cdot \text{m}$.

Rotating torque sensor , Nano newton-meter, Torsion Wire, Torsion pendulum, Watchmaking

1. Introduction

There is a lack of readily-available solutions to measure or apply torques in the nano newton-meter (10^{-9} Nm) range. On one side, the most sensitive commercial instruments are limited to applications in the micro newton-meter (10^{-6} Nm) range (e.g. Lecureux Kuiper sensor/actuator with a resolution of $100 \cdot 10^{-9}$ Nm or ATI nano17 sensor with a resolution of $16 \cdot 10^{-9}$ Nm). On the other side, known devices with a sensitivity in the nano newton-meter range are based on complex MEMS that are not commercially available, necessitate advanced fabrication processes, and need adaptation to operate as actuators [1, 2].

The work presented here aims at bridging this gap by designing a dedicated experimental setup to be used either as a *static torque sensor* or as *rotating torque sensor* (in conjunction with an actuator), with, in both cases, a resolution in the nano newton-meter range. The measuring principle is similar to conventional optical rotating torque sensors [3]) (also called twist-type optical torque transducers [4]). The central novelty is that a long (1 meter range) thin (diameter of a few tens of micrometers) metallic wire is used instead of the relatively stiff torsion zone of the shaft of classical rotating torque sensors. This thin wire, which is naturally curly, is made straight by placing it vertically and suspending a mass at its lower extremity. The very low torsional stiffness of the wire enables reaching the specified torque resolution. Precisely determining the torsional stiffness of the wire itself is crucial to accurate torque measurement as shown below. This has been realized by using the suspended mass itself as the bob of a torsion pendulum and measuring the frequency of the latter. The torsion angle of the wire is measured optically.

The setup is based on commercial sensors, standard components and conventionally-machined parts.

The applicability of our setup in static mode is demonstrated by measuring the output torque of a mechanical watch gear train in order to evaluate its friction losses. This gear train was designed to drive a new type of two-degrees-of-freedom flexure-based time base called *IsoSpring* [5–7] whose high quality factor and high frequency require one order of magnitude lower driving torque than standard oscillators. In this case, the frictional losses in the gear train are of the same order as the driving torque (typically $10 \cdot 10^{-9}$ Nm) and need to be quantified precisely.

2. Experimental approach

2.1. Setup

The experimental setup (Fig. 1) consists of a torsion wire suspending a mass to a fixed gantry. The mass is coupled to the rotating crank whose torque is to be measured via a pair of interface pins transmitting the couple. The contact between the pin and crank via two contact points is such that a pure torque is transmitted, without overconstraints. The torque value is derived from the torsion angle of the suspension wire, knowing its torsional stiffness. In the *static torque sensor* configuration, the upper extremity of the wire is attached to a fixed gantry and the torsion angle is determined by measuring the rotation of the suspended mass. In the *rotating torque sensor* configuration, the upper extremity of the wire is attached coaxially to the shaft of a servomotor whose angular position is controlled so as to maintain a given angular offset with the suspended mass and hence continuously controlling the torsion angle of the wire, which results in a precisely known applied torque.

The angular position measurement of the suspended mass, which is the key parameter of this setup, is achieved using a laser distance sensor (Keyence type LK-H082) pointed towards radial grooves machined in the suspended mass (Fig. 1b). These grooves are 0.5 mm deep and have a periodic angular spacing of 20 degrees. The signal returned by the distance sensor as the mass rotates (Fig. 2) is processed to detect the edges of the grooves and the angular position is reconstructed incrementally. The principle is similar to that of the widely-used incremental optical encoder.

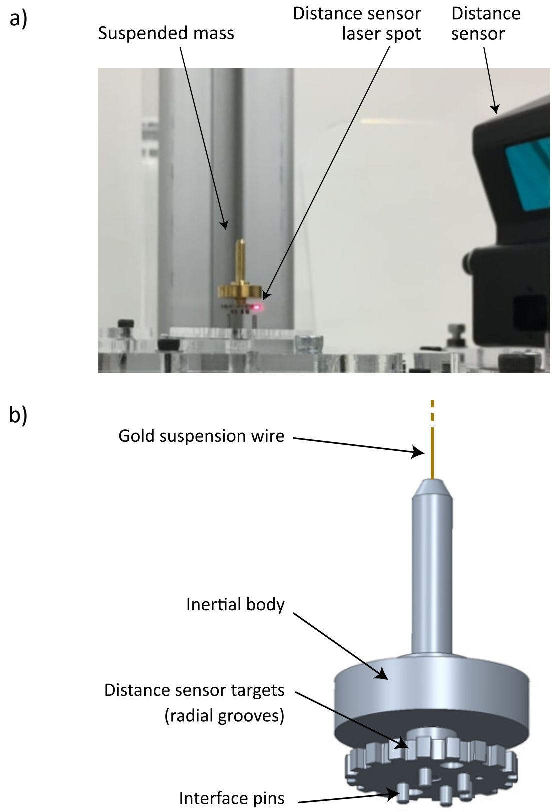

Figure 1. Nano-torque sensor/actuator experimental setup (a) and zoom on the suspended mass (b).

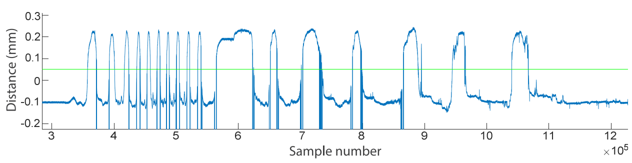

Figure 2. Distance sensor signal during the rotation of the mass.

Our setup uses a 99.99% gold wire (Heareus 4N bonding wire) with diameter $d = 38\ \mu\text{m}$ and length $L = 820\ \text{mm}$ chosen for its thinness, purity and low shear modulus. With a torsional stiffness $k_0 = 9.82\frac{\text{nN}\cdot\text{m}}{\text{rad}} = 61.7\frac{\text{nN}\cdot\text{m}}{\text{turn}}$ (characterized in Section 2.1) and an angular resolution $\alpha_r = 10° = 0.175\ \text{rad}$, the resulting torque resolution of the setup is $R = k_o\alpha_r = 1.71\ \text{nN}\cdot\text{m}$. For the range of torques considered for this sensor ($< 1\ \mu\text{N}\cdot\text{m}$), this resolution is the limiting factor to the accuracy of the setup. Indeed, in this range the uncertainty on the measured stiffness ($\pm 0.01\frac{\text{nN}\cdot\text{m}}{\text{rad}}$) results in an absolute torque uncertainty below $1.02\ \text{nN}\cdot\text{m}$.

2.2. Torsion wire characterization

In order to accurately estimate the torque resulting from the torsion of the suspension wire, it is essential to characterize its torsional stiffness. Knowing the moment of inertia of the suspended mass about the wire axis ($J = 21.8\ \text{g}\cdot\text{mm}^2$ obtained from the CAD file), the torsional stiffness of the wire was derived from the frequency of the system when it oscillates in torsion pendulum mode. For this, the suspended mass was released from an initial torsion angle and left to oscillate freely while its position is measured via the distance sensor. Figure 3 shows an extract of measurement data, where the groove edges and direction changes were detected by the signal processing algorithm. Note that the envelope of the signal shows perturbations that can be attributed to an imbalance of the rotating mass and oscillations in gravity pendulum mode. These are however enough distinct from the torsional frequency not to compromise the measurement.

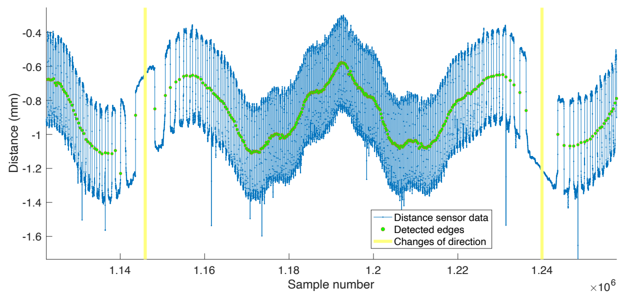

Figure 3. Angular position measurement of the suspended mass in free torsion pendulum oscillation (extract from a data set).

The position signal was sampled at 20 kHz, based on an OCXO quartz oscillator with a stability of ± 75 ppb (PXIe-6614) that allowed to precisely reconstruct the angular position of the oscillator over time (Fig. 4).

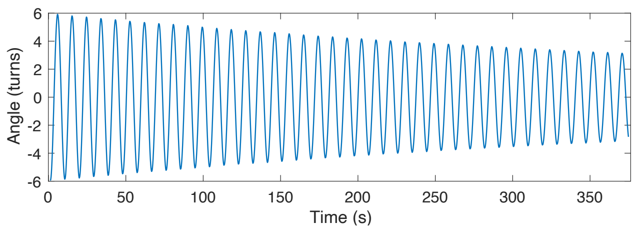

Figure 4. Reconstructed angular position vs time of the torsion pendulum.

In order to account for a potentially nonlinear torsional stiffness resulting in an amplitude-dependent oscillation frequency, we extracted the frequency-amplitude characteristic of the torsion pendulum (Fig. 5). This plot was obtained by fitting sinusoidal functions to subsets of the position versus time data with the algorithm described in our parallel research [8]. The nonlinear stiffness coefficients were then derived from the coefficients of a second order even polynomial fit of the frequency-amplitude characteristic: $\omega(\Theta) = \omega_0 + \omega_2\Theta^2$. Using the formula described in [9, Eq. 4-6], this yielded the nonlinear restoring torque

$$M = k_0\theta + k_2\theta^3 \tag{1}$$

where $k_0 = 9.82 \pm 0.01\frac{\text{nN}\cdot\text{m}}{\text{rad}}$ with 95% confidence intervals, $k_2 = (0.44 \pm 1.85)\cdot 10^{-5}\frac{\text{nN}\cdot\text{m}}{\text{rad}^3}$ and θ is the torsion angle. Note that the uncertainty on the inertia of the pendulum is considered smaller than that of the measurement and is hence not taken into account.

Since the upper bound of the nonlinear term k_2 would result in less than 0.4% stiffness increase for 6 turns (which corresponds to a $370\ \text{nN}\cdot\text{m}$ torque and is more than the requirements of our application in Section 3), it is reasonable to neglect it and assume a purely constant stiffness k_0. This is confirmed by the observation that the frequency variation with amplitude is within the measurement noise in Fig. 5 and is reflected in the uncertainty $(1.85 \cdot 10^{-5}\,\mathrm{nN} \cdot \mathrm{m/rad}^3)$ that is larger than the term itself $(0.44 \cdot 10^{-5}\,\mathrm{nN} \cdot \mathrm{m/rad}^3)$.

The measured torsional stiffness was validated with seven visual timings of the oscillation period using a stopwatch that returned an average period $T = 9.43\,\mathrm{s}$ with a standard deviation $\sigma = 0.36\,\mathrm{s}$. This corresponds to a mean stiffness of $9.66 \pm 0.68\,\frac{\mathrm{nN \cdot m}}{\mathrm{rad}}$ (with 95% confidence intervals) that matches our previous measurement.

We compared our stiffness measurements with theoretical estimations using the formula for the torsional stiffness of a bar with circular cross-section:

$$k = \frac{G\pi d^4}{32L} = 7.49\,\frac{\mathrm{nN} \cdot \mathrm{m}}{\mathrm{rad}} \qquad (2)$$

where $G = 30\,\mathrm{Gpa}$ is the shear modulus of gold. The 24% discrepancy with the experimental results shows the importance of properly measuring the effective stiffness in order to realize an accurate setup.

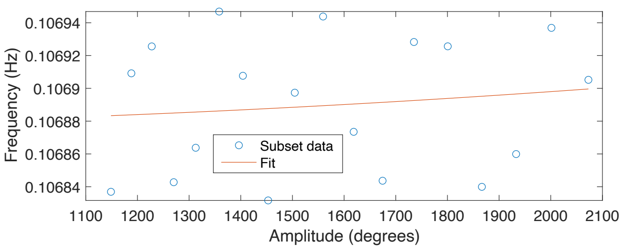

Figure 5. Measured frequency-amplitude data of the torsion pendulum.

3. Application example

The nano-torque sensor presented here was used to measure the frictional losses of a mechanical watch gear train dedicated to driving a silicon *IsoSpring* oscillator (see video in [7]). This oscillator has a higher frequency than classical mechanical watch oscillators (15 Hz vs 3 to 5 Hz) and a higher quality factor ($Q \approx 1000$ vs $Q \approx 200$) and thus requires a significantly lower driving torque ($20\,\mathrm{nN} \cdot \mathrm{m}$ vs typically $800\,\mathrm{nN} \cdot \mathrm{m}$ for the escape wheel of conventional mechanical watches). An off-the shelf watch movement “ETA Caliber 6497-1” has been modified by adding an extra gear stage in order to reduce the torque to the desired level. In this modified movement, as the output torque level is decreased, the fluctuation of the friction losses in the gear trains are relatively increased: they reach the same order of magnitude as the targeted useable torque itself. The ultimate aim of the experimental setup is to allow for an accurate characterization of these non-negligible losses.

These losses can be modelled as

$$T_{\mathrm{out}} = \frac{\eta}{i} T_{\mathrm{in}} - c_S\,\dot{\theta} - T_{\mathrm{const}} \qquad (2)$$

where T_{in} is the input torque, i is the total gear ratio, η is the load-dependent efficiency (mostly dependent on the friction between the gear teeth), c_S is the velocity-dependent loss coefficient, and T_{const} represents the constant losses (principally caused by the friction in the bearings of the gear train) [10]. Equation 2 shows that the load-dependent efficiency η and constant losses T_{const} can be determined from static measurements ($\dot{\theta} = 0$). Indeed, given the gear ratio, these coefficients define the slope and intercept of the static input-output torque characteristic. For this purpose, a sensor capable of measuring output torques of order $10 \cdot 10^{-9}\,\mathrm{Nm}$ was required.

The setup used to obtain the input-output torque characteristic of the modified gear train is depicted on Fig. 6. Various values of quasi-static input torque (in the micro newton-meter range) were applied with the Kuiper actuator and the output torque (in the nano newton-meter range) was measured with our experimental setup. The input is applied at the shaft of the fourth wheel (second hand shaft) via a crank, hence bypassing the upstream gear stages of the watch movement. The escape wheel (driven by the fourth wheel with a gear ratio 10:1) is replaced by an extra gear wheel engaging in an extra pinion with an gear ratio of 10:1. This results in a total gear ratio $i = 10 \cdot 10 = 100$ (i.e. the rotating speed is multiplied by 100) between input and output. The experimental results (Fig. 7) match the modelled linear characteristic and the desired physical quantities were obtained from the linear regression. The linear input to output torque ratio is 108, corresponding to a load-dependent efficiency of $\eta = 92.6\%$, with outputs torques ranging from $40 \cdot 10^{-9}$ to $160 \cdot 10^{-9}\,\mathrm{Nm}$. The estimated constant losses are $T_{\mathrm{const}} = 7.63\,\mathrm{nN} \cdot \mathrm{m}$.

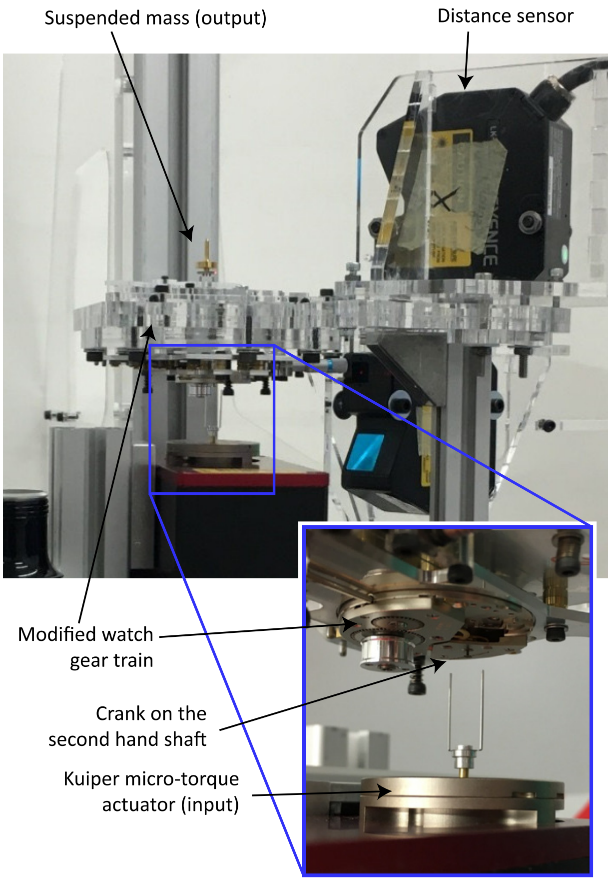

Figure 6. Setup for the static measurement of the modified mechanical watch gear train transmitted torque. Note: The torsion wire on which the mass is suspended is too thin to be visible.

Once these coefficients are known, the speed-dependent losses can be determined from the velocity of the gear train operating at constant velocity without output load ($T_{\mathrm{out}} = 0$) using Eq. 2:

$$c_S = \frac{\frac{\eta}{i} T_{\mathrm{in}} - T_{\mathrm{const}}}{\dot{\theta}} \qquad (3)$$

Note that, since the IsoSpring operates continuously, as opposed to the back and forth motion of traditional a 1-DOF oscillator, and at a higher frequency, the speed dependent losses are much greater.

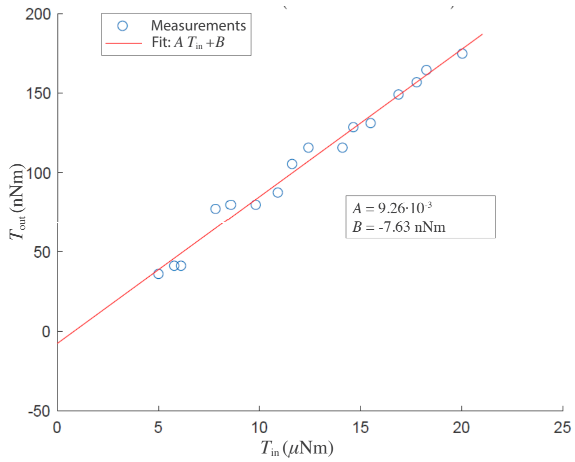

Figure 7. Measured input-output torque characteristic of the modified mechanical watch gear train.

4. Conclusion

A new experimental setup was developed to measure, statically or in rotation, torques in the nano newton-meter $(10^{-9}\ \mathrm{Nm})$ range. The theoretical resolution of the realized setup is $1.7 \cdot 10^{-9}\ \mathrm{Nm}$. Its appplicability was demonstrated in quasi-static mode by measuring the output torque of a modified mechanical watch two stage speed multiplying (100:1) gear train driven by a commercial torque meter. The range and resolution of the setup can be adapted by modifying the dimensions and material of the suspension of the wire whose length is limited solely by the vertical space available in the laboratory, as well as the number of grooves on the suspended mass. Additionally, a second distance sensor aimed at the grooves with an offset creating a quadrature signal could be used to double the angular resolution without modifying the rest of the setup.

We expect this instrument to become a benchmark for the experimental characterization of low torque micromechanical systems such as gear trains, bearings and flexure hinges. In future work, we will build upon the static results presented here to measure the dynamic losses of the studied gear train.

Acknowledgements

The authors thank Arnaud Maurel for his precious assistance in the design and implementation of the experimental setup.

References

[1] Brugger J et al., 1999, Microfabricated ultrasensitive piezoresistive cantilevers for torque magnetometry, *Sensors and Actuators A: Physical* **73**(3) 235–242; doi: 10.1016/S0924-4247(98)00240-4.

[2] Beyeler F et al., 2009, A Six-Axis MEMS Force–Torque Sensor With Micro-Newton and Nano-Newtonmeter Resolution, *Journal of Microelectromechanical Systems* **18**(2) 433–441; doi: 10.1109/JMEMS.2009.2013387.

[3] Zappalá D et al., 2018, Non-intrusive torque measurement for rotating shafts using optical sensing of zebra-tapes, *Measurement Science and Technology* **29** 065207; doi:10.1088/1361-6501/aab74a

[4] Pantaleo A et al., 2006, An optical torque transducer for high-speed cutting, *Measurement Science and Technology* **17** 331–339; doi:10.1088/0957-0233/17/2/014

[5] Rubbert L et al., 2016, Isotropic springs based on parallel flexure stages, *Precision Engineering* **43** 132–145; doi:10.1016/j.precisioneng.2015.07.003

[6] Vardi I et al., 2018. Theory and design of spherical oscillator mechanisms. *Precision Engineering* **51** 499–513; doi:10.1016/j.precisioneng.2017.10.005

[7] H. Schneegans et al., 2020, Driven Wattwins: a 2-DOF isotropic horological oscillator [Video files]; doi:10.5281/485zenodo.4309695.

[8] Thalmann E and Henein S, 2021, Optical Measurement Method for Mechanical Time Base Characterization, *euspen's 21st International Conference & Exhibition.*

[9] Thalmann E et al., 2020, Flexure Pivot Oscillator with Intrinsically Tuned Isochronism, *Journal of Mechanical Design* **142** (7); doi: 10.1115/1.4045388.

[10] Defossez L, 1950, Théorie générale de l'horlogerie. Chambre suisse de l'horlogerie.